

## Supplemental Figures

		<u>NLS</u>	
mouse	MSRRSQRLT--RYS-QDDNDGGSSSS-GASSVAGSQGTVFKDSPLRTLKRKSSNMKHLSP		56
rat	MSRRSQRLT--RYS-QDDNDG-SSSS-GASSVAGGQSTVFKDSPLRTLKRKSSNMKRLSP		55
human	MSRRSQRLT--RYS-QGDDDDGSSSS--GGSSVAGSQSTLTKDSPLRTLKRKSSNMKRLSP		55
chimpanzee	MSRRSQRLT--RYS-QGDDDDGSSSS--GGSSVAGSQSTLTKDSPLRTLKRKSSNMKRLSP		55
dog	MSRRSQRLT--RYS-QGDDDDGSSSS--GGSSVMGSQSTLTKDSPLRTLKRKSSNMKRLSP		55
horse	MSRRSQRLT--RYS-QGDDDDGSSSS--GGSSVMGSQSTLTKDSPLRTLKRKSSNMKRLSP		55
bovine	MSRRSQRLT--RYSSQGEDDDGGSSSS--GGSSVMGSQSTLTKDSPLRTLKRKSSNMKRLSP		57
opossum	MSRRSQRLI--RYS-QGDDDDGSSSSSSSSSLMIGQHVPFKDSPLRALRRKSSGMKRLSP		57
platypus	MSRRSQRLK--RYS-QGDDDDGSSSS--GGSSLVGSQHSFLFKDSPIRTLKRKSSNMKRLSP		56
zebra	MSRRSQRLVTTRY-PGDEDAITSSS--STSLGGTQLPFKEFTGRTIRKSSSTKRLSP		57
	***** ** ..:*. :** ..: . **:. *:::*. :*::**		
		<u>ER</u>	
mouse	APQLGPSSDSHTSYSESVVRESYIGSPRAVSLARSALLDDHLH-SEPYWSDLRGRRRR		115
rat	APQLPPPSDSHTSYSESVVRESYIGSPRAVSLARSALLDDHLH-SEPYWSDLRGRRRR		114
human	APQLGPSSDAHTSYSESLVHESWFP-PRS-----SLEELH-GDANWGEDLRVRRR		105
chimpanzee	APQLGPSSDAHTSYSESLVRESWFP-PRS-----SLEELH-GDANWGEDLRVRRR		105
dog	APQLGPSSDAHTSYSESVVRESYFSGPRAASLARSSILDDHLH-GDPYWSEDLRVRRR		114
horse	APQLGPSSDAHTSYSESVVRESYIGSPRAAALARSSIFDDQLH-GDSYWSEDLRVRRR		114
bovine	APQLGPSSDTHT-YYSESVVRESYIGSPRAASIA-ASLTHSLL-DDPYWSEDLRVRRR		114
opossum	APHLGSAKPHTSYSESVVSESYGRFRAPSVTKSSILHEQLD-SDSSWSDLMVGRR		116
platypus	APHLGTSSNTHTYSESMVSESYVGGPRSSPLARSSILHDDQDSDLYWNEDLRVRRR		116
zebra	TP-----STQTSYSESMSESYLGGSRGLPALGRSLDDDL-D-SSTYWGELSTRRR		110
	:* ..:* *****: **:* *. . . . . *:* . . . * * *		
		<u>INM?</u>	
mouse	GTGGSSESKANGLTAESKASEDFFGSSSGYSEEDDLAGYTDSDQHSSGSRLSAASRAGS		175
rat	GTGGSSESKANGLTMENKASEDFFGSSSGYSEEDDLAGYTDSDQHSSGSRLSAASRAGS		174
human	GTGGSSESRASGLV-GRKATEDFLGSSSGYSEEDDYVGYSDVDQSSSSRLSAVSRAGS		164
chimpanzee	GTGGSSESRASGLV-GRKATEDFLGSSSGYSEEDDYVGYSDVDQSSSSRLSAVSRAGS		164
dog	GTGGTESSKLNGLA-EDKSEDFLGGSSGYSEEDDFAGYSETDHRSSGSRLSNAVSWAAS		173
horse	GTGGTESSKINGLA-ENKLEDFFGSSSGYSEEDDYAGYSETDQRSSGSRLSAVSRAGS		173
bovine	GTGGTDSKPNGLP-ENKLEDFLGGSSGYSEEDDYVGYSETDHQSSGSRLSNAVSRVGS		173
opossum	GIGGPESKINMQT-EDKISYDTYGGSSGYSEEDDYSG---MDQPSVSRLSNAFFQAGA		172
platypus	DTGGTESSKINGLT-ENKVITYDTYGGSSGYSEEDDYTGHLGEDQYSSGSRLKKAASRAGS		175
zebra	GTGDTESSKINGVL--ESKTYDTYTSSSGYSEEDDYAGHYSGSSGSRLSNAVSRVGS		168
	. *..:***: . . : * ***** * . : * * * * . . .		
		<u>INM?</u>	
mouse	FVWTLVTFPGRLFGLLYWVGTWYRLTTAASLLDVFLVTRSRHFSLNLSKFL----		228
rat	FVWTLVTLPGRLFGLLYWVGTWYRLTTAASLLDVFLVTRSRHFSPNLSKFL----		227
human	LLWMVATSPGRLFRLLYWAGTWTWYRLTTAASLLDVFLVTR--RFSS-LKTFL----		214
chimpanzee	LLWMVATSPGRLFRLLYWAGTWTWYRLTTAASLLDVFLVTR--RFSS-LKTFL----		214
dog	CFWMVVTSPGRLFGLLYWVGTWYRLTTAASLLDVFLVTR--RFSS-VKTFL----		223
horse	FFWMVVTSPGRLFGLLYWVGTWYRLTTAASLLDVFLVTR--RFSS-LKTFL----		223
bovine	LLWMVVTSPGRLFGLLYWVGTWYRLTTAASLLDVFLVTR--RFSS-LKMF----		223
opossum	FLWMVVTSPGRLFGLLYWVGTWYRLTTAASLLDVFLVTR--CFAS-LKKLLSFL		226
platypus	FLWMVVTSPGQLFGLCYWVGTWYRLTTAASLLDVFLVTR--RFPS-LK-----		222
zebra	FLWQVFTSPVQLLRWLFSGLAGAWRLTGTASHLDNVFSSR--RYPR-LKRSL----		218
	. * : * * * : : . : * * * * * * * . : : * : . : *		

**Figure S1.**

### Sequence alignment of SUN2 from different vertebrate species.

ClustalW sequence alignment of the N-terminal domains of SUN2 family members from *Mus musculus* (mouse), *Rattus norvegicus* (rat), *Homo sapiens* (human), *Pan troglodytes* (chimpanzee), *Canis familiaris* (dog), *Equus caballus* (horse), *Bos taurus* (bovine), *Monodelphis domestica* (opossum), *Ornithorhynchus anatinus* (platypus), *Taeniopygia guttata* (zebra finch). The sequence motifs under investigation in this study are indicated on top of the alignment. NLS - nuclear localization signal, ER - Arg-based ER localization signal.

SUN2 also contains sequence elements resembling inner nuclear membrane sorting motifs (INM-SMs, Braunagel et al, 2004). INM-SMs are characterized by positively charged amino acids located 4 to 8 amino acids away from the nucleoplasmic face of a transmembrane domain. We spotted three such potential INM-SMs in SUN2, indicated by 'INM?', one of it preceding the transmembrane domain (R205/R206), and two others preceding hydrophobic stretches in SUN2 (R175/R178; R154/R156). INM? - putative inner nuclear membrane sorting motif.

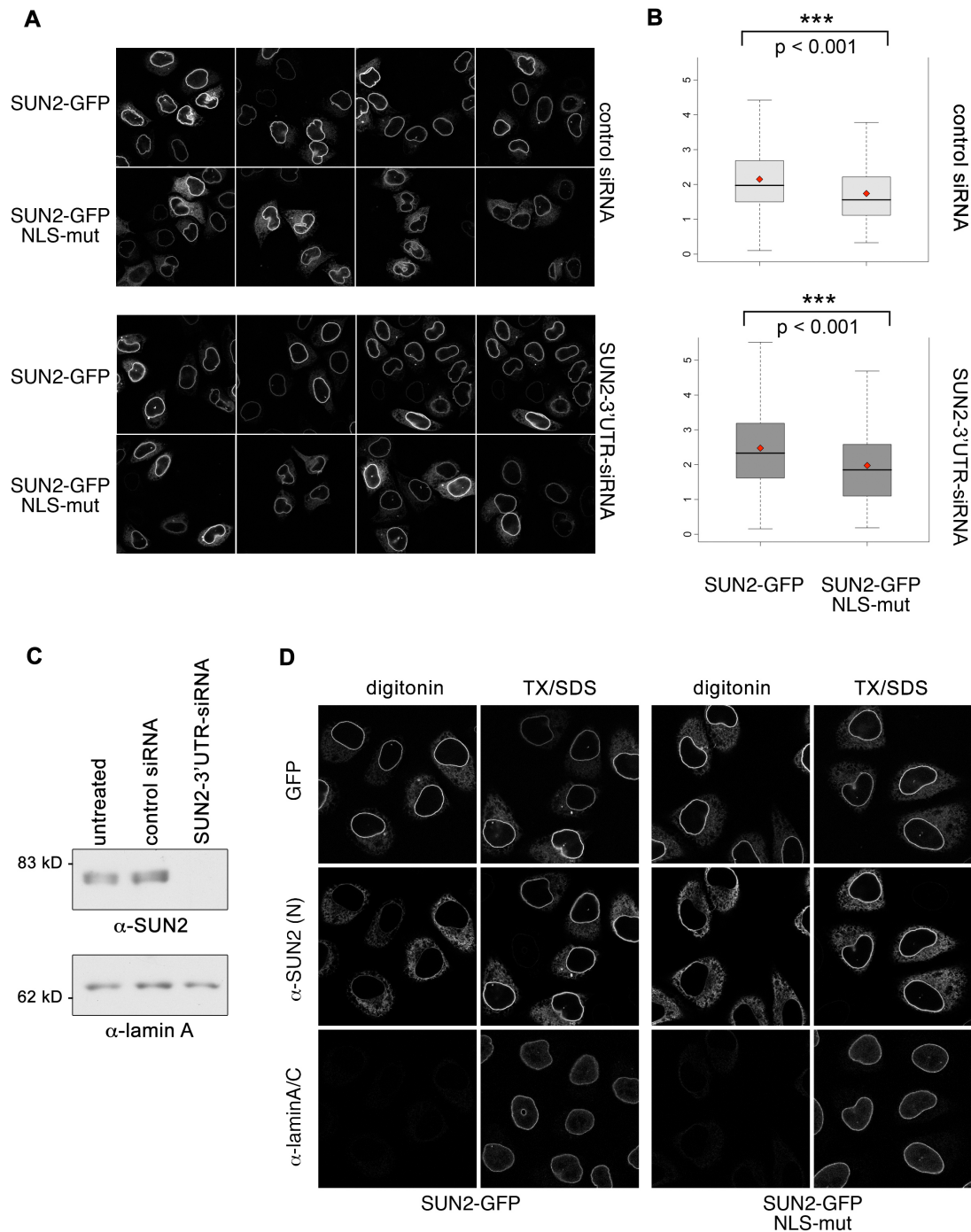


**Figure S2.**

**Mutation of the basic NLS in the N terminus of SUN2 only slightly affects NE localization.**

A) HeLa cells were treated with either control or SUN2 3'UTR siRNA for 48 h and then transfected with wild-type or the NLS mutant of SUN2-GFP. Cells were fixed 24 h later, stained with Hoechst (not shown) and analyzed by confocal fluorescence microscopy. Note that the NLS mutation in SUN2-GFP(NLS-mut) does not abolish NE targeting but slightly enhances ER localization compared to wild-type SUN2-GFP.

B) Quantification of 'NE' over 'ER' localization of the experiment presented in (A). To provide a numerical description of the NE to ER ratio of wild-type SUN2-GFP and SUN2-GFP(NLS-mut), confocal images were subjected to automated analysis using a MATLAB-based image

analysis software. Each value represents the mean NE/ER ratio of three independent experiments, obtained from 450-1000 cells, +/- SEM. Statistical analysis was performed with the software R using the Welch's t-test. Note that the NE/ER ratio of the transmembrane domain of SUN2 (GFP-SUN2(213-260)), which does not enrich at the NE, is <1.2 (not shown).

(C) Efficient downregulation of SUN2 after RNAi. HeLa cells were left untreated or treated with siRNAs as in (A). 72 h after transfection, cells were harvested, washed, lysed in SDS sample buffer and analyzed by SDS-PAGE/Western blotting using the indicated antibodies.

(D) SUN2-GFP(NLS-mut) reaches the INM. Cells were transfected as in (A). After 24 h, cells were fixed and permeabilized with either only digitonin or subsequently also with Triton X-100/SDS (TX/SDS). Immunostaining was performed using a mouse anti-laminA/C antibody, detected by an Alexa633-labeled secondary antibody, and an anti-SUN2(N) antibody recognizing the N-terminal 158 aa of SUN2, detected by an Alexa568-labeled secondary antibody. Scans were taken by confocal fluorescence microscopy by sequential scanning of GFP, Alexa568 and Alexa633. Note that endogenous SUN2 is not detected in non-transfected cells at the selected antibody concentration.

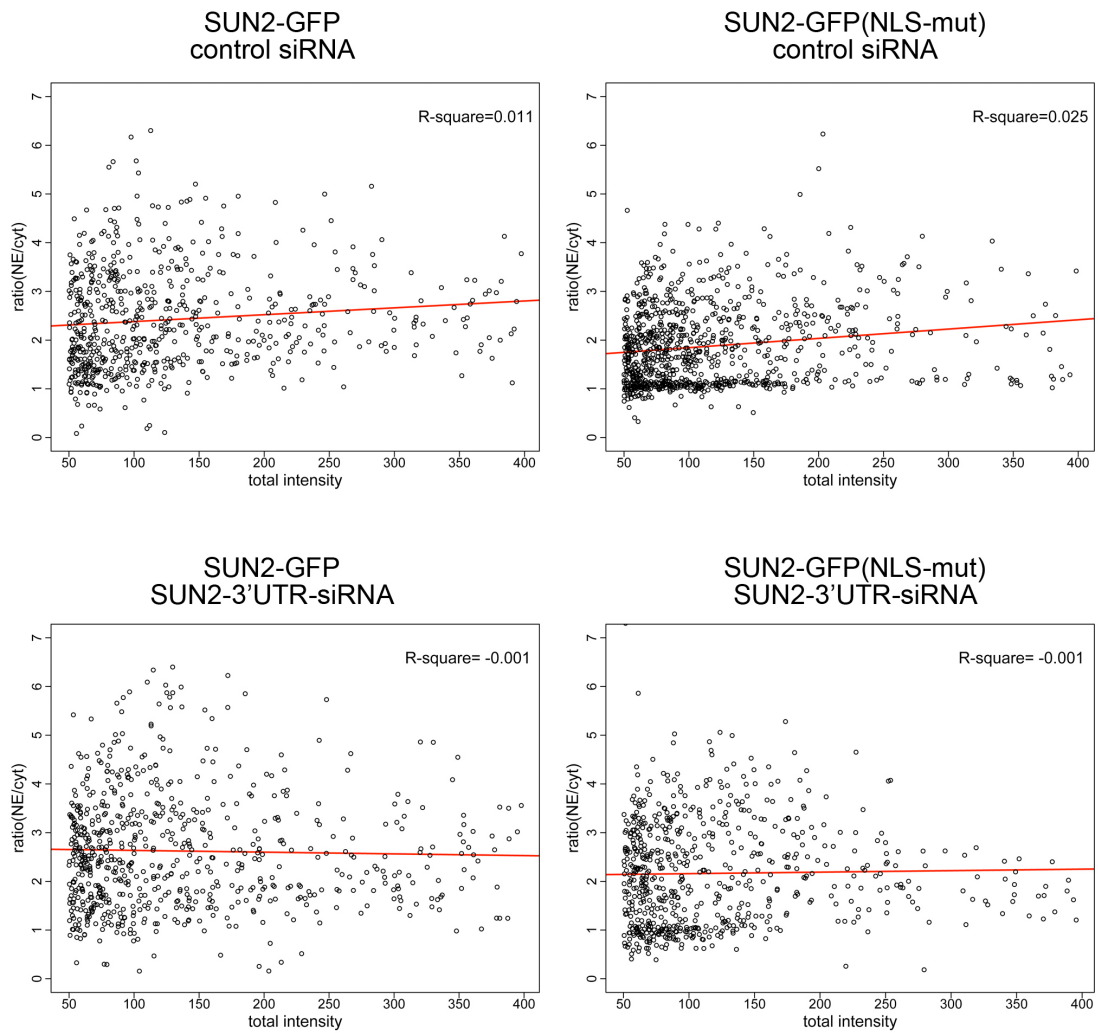


**Figure S3.**

**NE accumulation of SUN2-GFP does not correlate with expression levels.**

Correlation analysis of NE/ER ratios and expression levels (based on total fluorescence intensities) for the experiment presented in Figure S2. The NE/ER ratios are plotted over the total fluorescence intensities. The determination coefficient R-square represents the correlation of the variables.



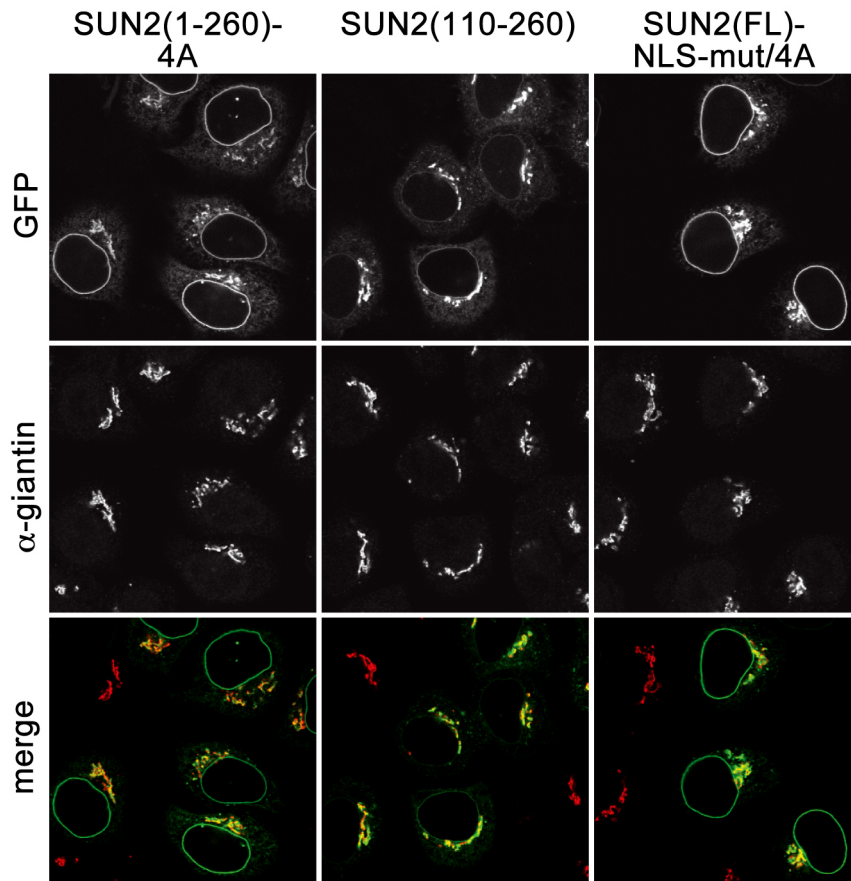


**Figure S4.**

**SUN2 derivatives deficient in the 4R Golgi retrieval signal accumulate in the Golgi apparatus.**

HeLa cells were transfected with the indicated C-terminal GFP-tagged derivatives of SUN2, namely SUN2(1-260)-4A, SUN2(110-260) or SUN2(FL)-NLS-mut/4A. Cells were fixed 24 h after transfection and immunostained using an antibody directed against the Golgi marker protein giantin, detected by an Alexa568-labeled secondary antibody. Scans were taken by confocal fluorescence microscopy by sequential scanning of GFP and Alexa568.

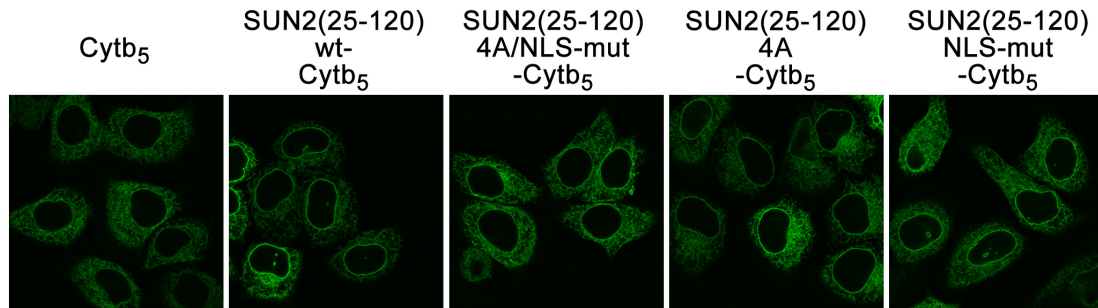


**Figure S5. An N-terminal fragment of SUN2 comprising the NLS and the 4R motif can enrich cytochrome b5 at the NE.**

HeLa cells were transfected with C-terminally GFP-tagged cytochrome b5 or the indicated derivatives bearing wild-type or mutated fragments of SUN2(25-120). Cells were fixed 48 h after transfection and analyzed by confocal fluorescence microscopy.

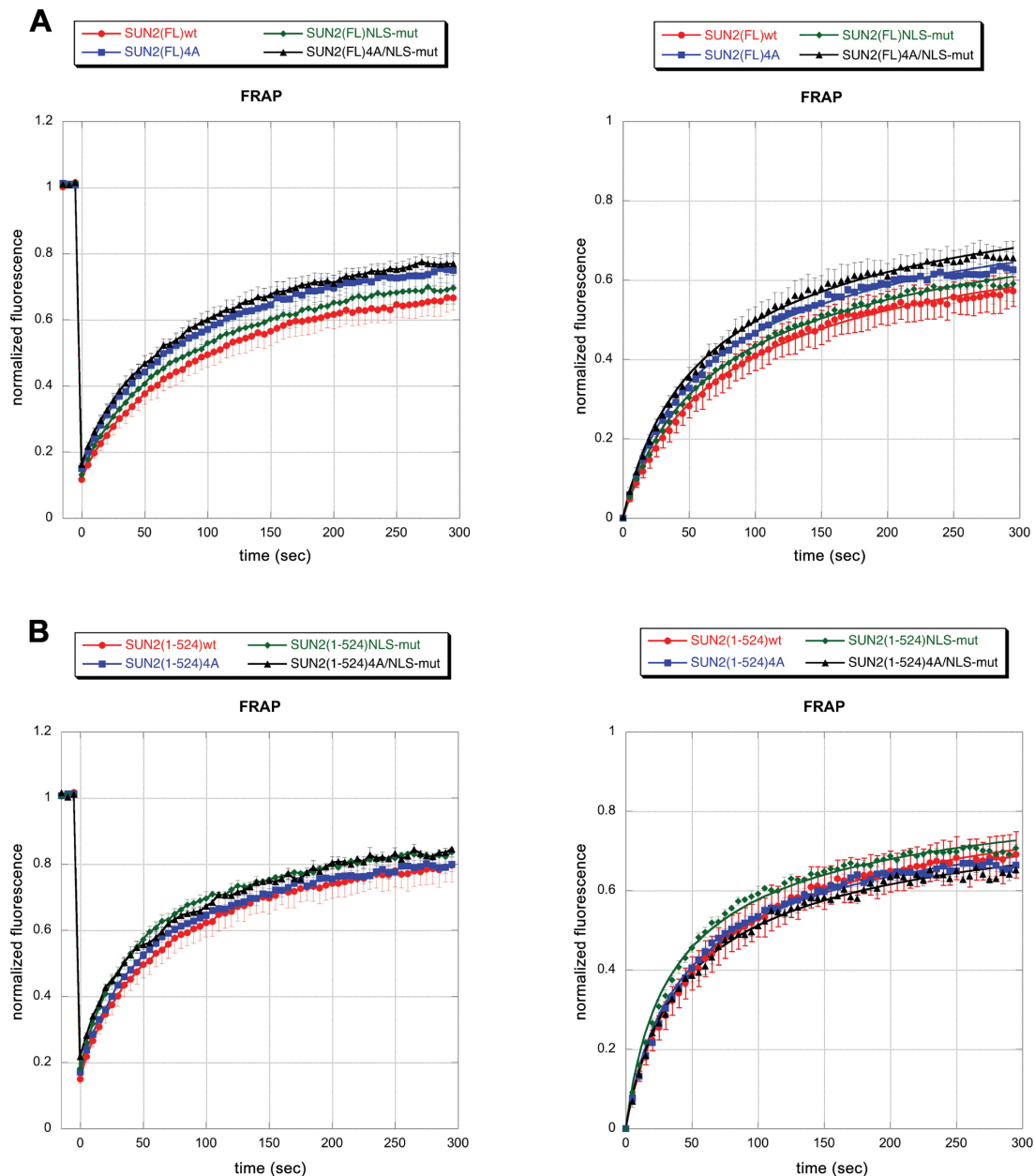


**Figure S6.**

**Mobility of SUN2 in the NE is not majorly affected by mutation of the NLS and/or the ER retrieval signal.**

FRAP analysis of the diffusional mobility of wild-type SUN2(FL)-GFP (A) and SUN2(1-524)-GFP (B) and their indicated mutants at the NE in transiently transfected HeLa cells. GFP fluorescence was bleached within a defined region of 1.4  $\mu\text{m}$  x 3.5  $\mu\text{m}$ . Fluorescence recovery was monitored for 300 s in 5 s intervals. Experimental data were normalized, and corrected for background signal and bleaching during image acquisition. Recovery of the fluorescence intensity of each GFP construct represents the mean of 3 x 10 independent measurements and was plotted as a function of time +/- SEM. The data were fitted as previously described (Ellenberg et al., 1997). On the left hand panels, the pre-bleach fluorescence is shown, on the right hand panels, fluorescence was additionally normalized to post-bleach fluorescence. Note that for the FRAP experiments, cells of different expression levels were used as judged based on the intensities of the GFP signal.

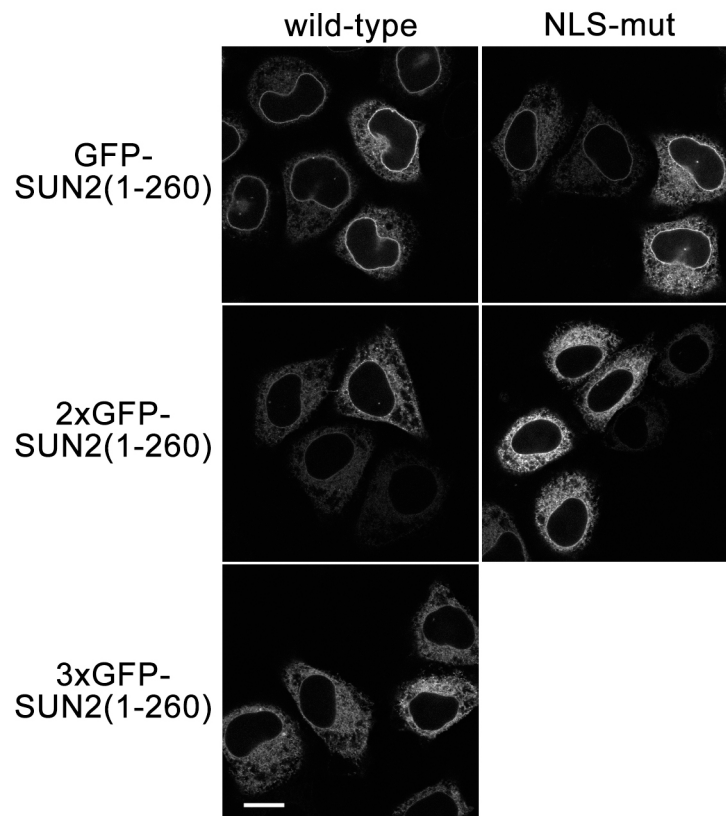


**Figure S7.**

**Increasing the size of the N-terminal domain of SUN2 abolishes NE targeting.**

HeLa cells were transfected with the indicated derivatives of GFP-SUN2(1-260), 2xGFP-SUN2(1-260) and 3xGFP-SUN2(1-260). Cells were fixed 24 h after transfection and analyzed by confocal fluorescence microscopy. Scale bar is 15  $\mu$ m. Note that 3xGFP-SUN2(1-260) fails to be enriched at the nuclear rim.

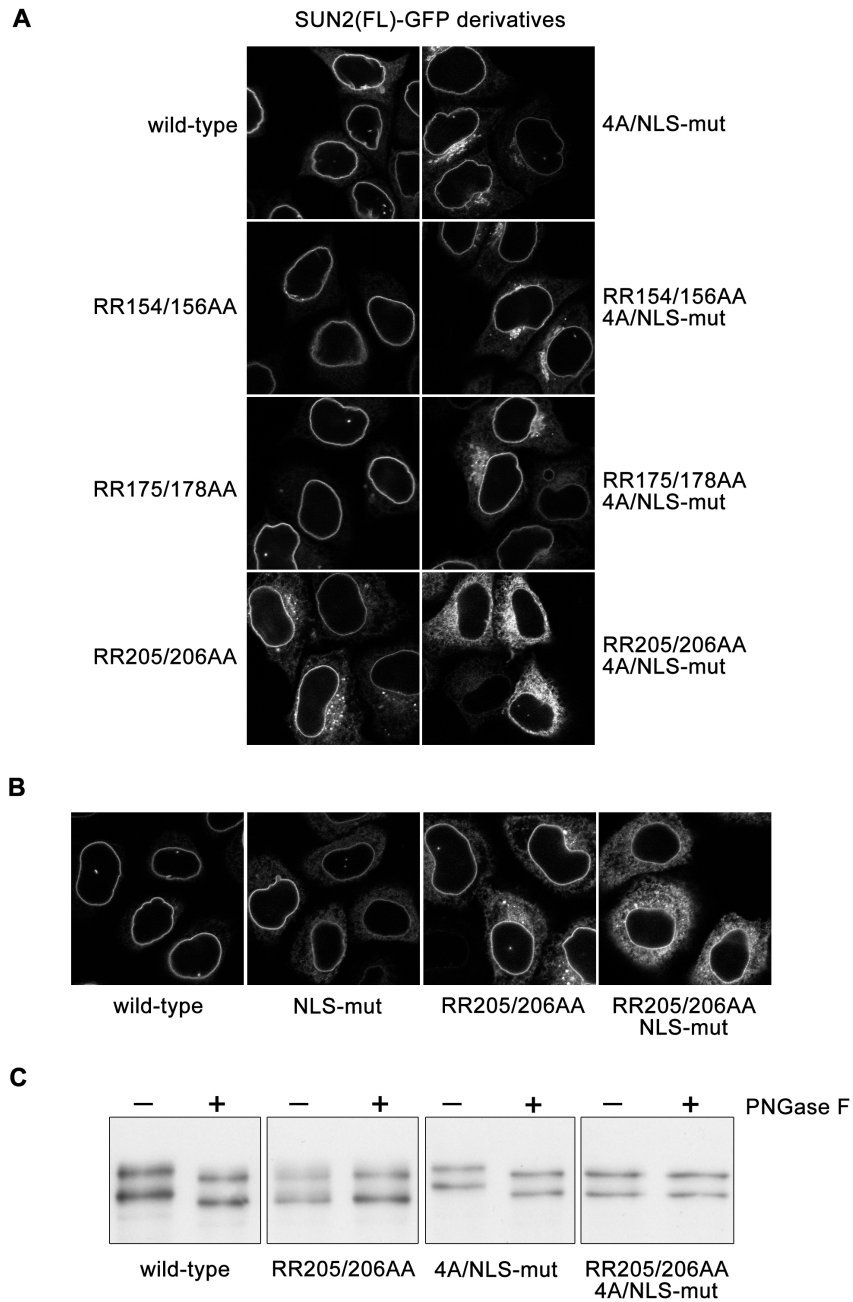


**Figure S8.**

**Analysis of the contribution of three different, potential INM sorting motifs in SUN2 to NE targeting.**

(A) HeLa cells were transfected with the indicated derivatives of SUN2(FL)-GFP. Cells were fixed 24 h after transfection and analyzed by confocal fluorescence microscopy. In the RR205/206AA mutant, the orientation of the SUN domain is disturbed such that it faces the cytoplasm instead of the perinuclear space (see C). Note that combination of the mutations in the NLS/4R and the RR205/206 completely prevents NE enrichment of the reporter underscoring the importance of both the SUN domain and the identified sequence elements in the N-terminal domain of SUN2 for INM targeting.

(B) Experiment as in (A) including the combination of mutations in the SUN2-NLS and RR205/206AA. Note the strong NE targeting defect upon combination of the NLS and RR205/206 mutations.



(C) Mutation of RR205/206 in SUN2 to alanines changes the membrane orientation of the C-terminal domain. HeLa cells were transfected with the indicated constructs. After 24 h, cells were lysed in deglycosylation buffer and subjected to either mock treatment (-) or treatment with PNGase F (+). The glycosylation status of position 636 in the C-terminal domain of SUN2 was determined by examining the mobility of the GFP-tagged SUN2 derivatives in immunoblot using antibodies directed to GFP. A similar analysis for SUN2(RR154/156AA)-GFP and SUN2(RR175/178AA)-GFP revealed a correct orientation of the C-terminal domain for these mutant proteins (data not shown).

## Supplemental Material and Methods

### *Molecular Cloning*

For domain swap experiments, the cytochrome b5 coding region was amplified from a rat full-length cDNA clone (pSVb5) kindly provided by A. Ito (Mitoma and Ito, 1992) and cloned into the EcoRI/Sall sites of pEGFP-N3. N-terminal fusions with SUN2(25-120) wild-type or mutant derivatives were generated using BglII/EcoRI sites. For expression of N-terminally xGFP-tagged SUN2(1-260) fusions, PCR fragments obtained from SUN2(FL) or pEGFP-C1-SUN2(FL) were subcloned into pEGFP-C2 or pEGFP<sub>2</sub>-C2 (kindly provided by Dr. G. Rabut, ETH Zurich) using the EcoRI-BamHI sites to generate GFP-SUN2(1-260), 2xGFP-SUN2(1-260) and 3xGFP-SUN2(1-260). Putative INM sorting motifs in SUN2 were mutated using the QuikChange Mutagenesis Kit (Stratagene) generating the following changes: R154A/R156A; R175A/R178A; R205A/R206A.

### *Deglycosylation*

HeLa cells were lysed in deglycosylation buffer (0.5% SDS, 40 mM DTT, 2 mM PMSF). The cell lysates were cleared by centrifugation at 13'000 rpm at 4°C in a table centrifuge and processed with or without PNGase F (New England Biolabs) according to the manufacturer's instructions.

### *Fluorescence Recovery after Photobleaching (FRAP)*

FRAP experiments were performed on a 37°C stage of a LSM 510-Screening confocal microscope, using an oil-immersion objective (PlanApochromat 63x/1.4 Oil). GFP fluorescence was bleached (500 iterations) by the 488 nm line at full laser power within a defined region of 1.4 μm x 3.5 μm. Fluorescence recovery was monitored at lower laser power (10 %; 512x512 pixels; 4 x zoom; scan time 1.6 μs). The effective length (4 μm and accordingly 1.9 μm x 4 μm for the rectangle) and entire depth of the bleached area was measured by photobleaching of fixed cells under the same conditions. Experimental data were normalized, the background subtracted and corrected for bleaching during image acquisition.

### *Antibodies*

Mouse monoclonal antibodies against lamin A, lamin A/C and β-actin were purchased from Novacastra, Abcam and Sigma, respectively. Rabbit polyclonal antibody against giantin was purchased from Covance. Polyclonal antibodies to human SUN2 and GFP were generated by immunization of rabbits with antigens comprising aa 1-158 of SUN2 or full-length recombinant GFP.

### *Cell culture, transient transfections and RNAi*

HeLa cells were maintained in DMEM containing 10% FCS and penicillin/streptomycin at 37°C, 5% CO<sub>2</sub>. Transient transfections were done using FuGene transfection reagent (Roche), according to the manufacturers protocol. Cells were fixed 24 to 36 hours after transfection with 4% PFA for 10 min. Hoechst staining was performed with 1 μg/ml Hoechst for 5 min. After washing with PBS, cover slips were mounted in VectaShield (VectorLabs) for microscopic analysis.

For RNAi experiments, the following siRNAs (17.5 nM) were used: SUN2-3'UTR (5'-GCTAAGGGCTTGATTCCTAdTdT-3'); AllStar negative control (Qiagen). Transfection of siRNAs was done with Oligofectamine (Invitrogen). After 48 hours of RNAi, cells were transfected with plasmid DNA encoding SUN2-GFP fusions and incubated for another 24 hours before fixation.

#### *Microscopy, image analysis and quantification*

Confocal microscopy was performed with a Leica TCS-SP2/AOBS microscope using a HCX PI APO lbd.BI. 40x, NA 1.25 or HCX PI APO lbd.BI. 63x, NA 1.4 oil immersion lens or with a Leica TCS-SP1 microscope using a HCX PI APO lbd.BI. 40x, NA 1.25 or HCX PI APO lbd.BI. 63x, NA 1.32 oil immersion lens. Images were analyzed in the sequential scan mode, using the 405 nm diode for detection of Hoechst dye. GFP was analyzed using the 488 nm laser line of an argon laser.

To determine the NE/ER ratio of wild-type SUN-GFP and SUN-GFP(NLS-mut), cell nuclei were detected based on the blue Hoechst fluorescence using adaptive thresholding and the Watershed algorithm to separate touching cells. To obtain a quantitative readout for NE over ER fluorescence for each cell, two adjacent rings were defined surrounding the cell nucleus. The 'NE' ring was 1098 nm wide (3 pixels), reaching to 66% (2 pixels) into the nucleus (overlap with Hoechst), whereas 33% of the ring covered an area outside the Hoechst staining (1 pixel) on the cytoplasmic side. The 'ER' ring was surrounding the NE ring and 12 pixels (4395 nm) wide. The NE/ER ratio was calculated by dividing the mean fluorescence intensities in both areas. Note that the absolute accumulation of SUN2 derivatives at the NE is underestimated because of the use of a ring of three pixels at the NE required to reliably include the NE-derived signal.

#### **Supplemental Citations:**

Braunagel SC, Williamson ST, Saksena S, Zhong Z, Russell WK, Russell DH, Summers MD (2004) Trafficking of ODV-E66 is mediated via a sorting motif and other viral proteins: facilitated trafficking to the inner nuclear membrane. *Proc Natl Acad Sci USA* **101**: 8372-8377

Ellenberg J, Siggia ED, Moreira JE, Smith CL, Presley JF, Worman HJ, Lippincott-Schwartz J (1997) Nuclear membrane dynamics and reassembly in living cells: targeting of an inner nuclear membrane protein in interphase and mitosis. *J Cell Biol* **138**: 1193-1206

Mitoma, A and Ito, A (1992) The carboxy-terminal 10 amino acid residues of cytochrome b5 are necessary for its targeting to the endoplasmic reticulum. *EMBO J.* **11**: 4197-4203